

Solution of Laminar Diffusion Flames Using a Parallel Adaptive Mesh Refinement Algorithm

S. A. Northrup* and C. P. T. Groth†

*University of Toronto Institute for Aerospace Studies
Toronto, Ontario, M3H 5T6, Canada*

A parallel block-based adaptive mesh refinement (AMR) scheme is developed and applied to the prediction of the structure of non-premixed axisymmetric methane-air laminar diffusion flames. The parallel solution-adaptive algorithm solves the system of partial-differential equations governing two-dimensional axisymmetric compressible laminar flows for reactive thermally perfect gaseous mixtures. A finite-volume spatial discretization procedure is used to solve the conservation form of the mixture continuity, momentum, and energy equations and species mass fraction equations on body-fitted multi-block quadrilateral mesh. The compressible formulation can readily accommodate large density variations and thermoacoustic phenomena. A local preconditioning technique is used to remove numerical stiffness and maintain solution accuracy for low-Mach-number, nearly incompressible flows. Limited piecewise linear solution reconstruction and Riemann solver based flux functions are used in the evaluation of inviscid fluxes and a centrally weighted second-order discretization procedure is adopted for determining the viscous fluxes. A flexible block-based hierarchical data structure is used to facilitate mesh adaptation according to physics-based refinement criteria. The data structure also enables efficient and scalable implementations of the algorithm on multi-processor architectures via domain decomposition. Numerical results are discussed for co-flow laminar diffusion flames. The validity of the parallel AMR approach and the ability of the mesh adaptation scheme to resolve fine-scale features of laminar flames is demonstrated.

I. Introduction

Combustion refers to the complex physical/chemical processes by which a fuel and oxidizer undergo irreversible chemical reactions to produce heat. It is one of the most widely experienced phenomena in nature and occurs in or is a key component of many of practical technologies that directly impact society today including aircraft and rocket engines for transportation and propulsion. In spite of this, there are many unresolved issues associated with our understanding of and ability to predict combustion phenomena. Over the last 10-15 years, the application of computational fluid dynamics (CFD) methods to reactive flows has yielded an improved understanding of combustion processes. Nevertheless, combustion involves a wide range of complicated physical and chemical phenomena (flame behaviour is dictated by a strong interaction between the flow structure, chemical kinetics, and thermodynamic properties of the reactants and products), each with their own characteristic spatial and/or temporal scales. In many cases, combusting flows exhibit large disparities in these characteristic scales and the solution of such flows places heavy demands on cur-

*PhD Candidate, Student Member AIAA, northrup@utias.utoronto.ca

†Associate Professor, Senior Member AIAA, groth@utias.utoronto.ca

rently available computing resources. For these reasons, the prediction of combustion processes by numerical methods remains a very challenging area of research.

Many approaches have been taken to reduce the computational costs of performing simulations of combustng flows. One successful approach is to make use of solution-directed mesh adaptation, such as the adaptive mesh refinement (AMR) algorithms developed for aerodynamic flows.^{1–11} Computational grids that automatically adapt to the solution of the governing equations are very effective in treating problems with disparate length scales, providing the required spatial resolution while minimizing memory and storage requirements. The work by Day and Bell¹² describes the application of an AMR algorithm to laminar diffusion flames. Another approach is to apply a domain decomposition procedure and solve the problem in parallel using multiple processors. Large massively parallel distributed-memory computers can provide many fold increases in processing power and memory resources beyond those of conventional single-processor computers and would therefore seem to provide an obvious avenue for greatly reducing the time required to obtain numerical solutions of combustng flows. Douglas *et al.*¹³ describe a parallel algorithm for numerical combustion modelling. The focus of the present study is to couple these two approaches, producing a method that both reduces the overall problem size and the time to calculate a solution for combustng flows.

A parallel block-based adaptive mesh refinement (AMR) scheme is described and applied to the prediction of the structure of non-premixed axisymmetric methane-air laminar diffusion flames. The parallel solution-adaptive algorithm solves the system of partial-differential equations governing two-dimensional axisymmetric compressible laminar flows for reactive thermally perfect gaseous mixtures. A finite-volume spatial discretization procedure is used to solve the conservation form of the mixture continuity, momentum, and energy equations and species mass fraction equations on body-fitted multi-block quadrilateral mesh. High-temperature thermodynamic and transport properties of the gaseous species are prescribed using the semi-empirical relations of Gordon and McBride.^{14,15} The compressible formulation can readily accommodate large density variations and thermoacoustic phenomena. A local preconditioning technique is used to remove numerical stiffness and maintain solution accuracy for low-Mach-number, nearly incompressible flows. Limited piecewise linear solution reconstruction and Riemann solver based flux functions are used in the evaluation of inviscid fluxes and a centrally weighted second-order discretization procedure is adopted for determining the viscous fluxes. A flexible block-based hierarchical data structure is used to facilitate mesh adaptation according to physics-based refinement criteria. The data structure also enables efficient and scalable implementations of the algorithm on multi-processor architectures via domain decomposition.

Details are provided concerning the finite-volume solution scheme, low-Mach-number local preconditioning technique, AMR strategy, and domain decomposition procedure. The parallel performance of the AMR algorithm is also discussed. Numerical results are described for both premixed and non-premixed laminar flames, including co-flow axisymmetric methane-air diffusion flames using a simple two-step reduced chemical kinetic scheme.¹⁶ The validity of the parallel AMR approach and the ability of the mesh adaption scheme to resolve the fine-scale features of laminar flames is demonstrated.

II. Mathematical Modelling

A. Navier Stokes Equations

The governing conservation equations describing the behaviour of a thermally perfect reactive gaseous mixture can be expressed as

$$\frac{\partial}{\partial t}(\rho) + \nabla \cdot (\rho \mathbf{U}) = 0, \quad (1)$$

$$\frac{\partial}{\partial t}(\rho \mathbf{U}) + \nabla \cdot (\rho \mathbf{U} \mathbf{U} + p \vec{\mathbf{I}}) = \nabla \cdot \vec{\tau} - \rho \mathbf{g}, \quad (2)$$

$$\frac{\partial}{\partial t} [\rho E] + \nabla \cdot \left[\rho \mathbf{U} \left(E + \frac{p}{\rho} \right) \right] = \nabla \cdot (\mathbf{U} \cdot \vec{\tau} - \mathbf{q}) - \rho \mathbf{g} \cdot \mathbf{U}, \quad (3)$$

$$\frac{\partial}{\partial t} (\rho c_s) + \nabla \cdot (\rho c_s \mathbf{U}) = \nabla \cdot (\rho D_s \nabla c_s) + \rho \dot{\omega}_s, \quad (4)$$

where Eqs. (1)–(3) reflect the conservation of mass, momentum, and energy for the reactive mixture, ρ is the mixture mass density, \mathbf{U} is the mixture velocity, E is the total specific energy of the mixture given by

$$E = e + \frac{1}{2} |\mathbf{U}|^2, \quad (5)$$

e is the specific internal energy, p is the mixture pressure, $\vec{\tau}$ is the fluid stress tensor for the mixture, \mathbf{q} is the heat flux vector, and \mathbf{g} is the acceleration due to gravitational forces. Equation (4) is the species concentration equation for species s , where c_s is the species mass fraction, D_s is the diffusion coefficient, and $\dot{\omega}_s$ is the time rate of change of the species concentration due to finite-rate chemistry. It follows from the caloric equation of state for a thermally perfect mixture that

$$e = \sum_{s=1}^N c_s h_s - \frac{p}{\rho}, \quad (6)$$

where h_s is the species enthalpy, N is the number of species, and the ideal gas law for the mixture is given by

$$p = \sum_{s=1}^N \rho c_s R_s T, \quad (7)$$

where R_s is the species gas constant and T is the mixture temperature. For two-dimensional axisymmetric flows, these equations can be re-expressed using vector notation as

$$\frac{\partial \mathbf{U}}{\partial t} + \frac{\partial \mathbf{F}}{\partial r} + \frac{\partial \mathbf{G}}{\partial z} = \frac{\partial \mathbf{F}_v}{\partial r} + \frac{\partial \mathbf{G}_v}{\partial z} + \frac{\mathbf{S}_a}{r} + \mathbf{S} \quad (8)$$

where \mathbf{U} is the vector of conserved variables given by

$$\mathbf{U} = \left[\rho, \rho U_r, \rho U_z, \rho E, \rho c_1, \dots, \rho c_N \right]^T, \quad (9)$$

\mathbf{S}_a and \mathbf{S} are source terms associated with the axisymmetric geometry, finite rate chemistry and gravitational forces, respectively, and have the form

$$\mathbf{S}_a = \begin{bmatrix} -\rho U_r \\ -\rho U_r U_r + \tau_{rr} - \tau_{\theta\theta} \\ -\rho U_r U_z + \tau_{rz} \\ -\rho U_r \left(E + \frac{p}{\rho} \right) + U_r \tau_{rr} + U_z \tau_{rz} - q_r \\ -\rho c_1 U_r + \rho D_1 \frac{\partial c_1}{\partial r} \\ \vdots \\ -\rho c_N U_r + \rho D_N \frac{\partial c_N}{\partial r} \end{bmatrix}, \quad \mathbf{S} = \begin{bmatrix} 0 \\ 0 \\ \rho g_z \\ \rho g_z U_z \\ \rho \dot{\omega}_1 \\ \vdots \\ \rho \dot{\omega}_N \end{bmatrix}, \quad (10)$$

the inviscid flux vectors, \mathbf{F} and \mathbf{G} , are

$$\mathbf{F} = \begin{bmatrix} \rho U_r \\ \rho U_r U_r + p \\ \rho U_z U_r \\ \rho U_r \left(E + \frac{p}{\rho} \right) \\ \rho c_1 U_r \\ \vdots \\ \rho c_N U_r \end{bmatrix}, \quad \mathbf{G} = \begin{bmatrix} \rho U_z \\ \rho U_r U_z \\ \rho U_z U_z + p \\ \rho U_z \left(E + \frac{p}{\rho} \right) \\ \rho c_1 U_z \\ \vdots \\ \rho c_N U_z \end{bmatrix}, \quad (11)$$

and the viscous flux vectors \mathbf{F}_v and \mathbf{G}_v are given by

$$\mathbf{F}_v = \begin{bmatrix} 0 \\ \tau_{rr} \\ \tau_{zr} \\ U_r \tau_{rr} + U_z \tau_{rz} - q_r \\ \rho \mathcal{D}_1 \frac{\partial c_1}{\partial r} \\ \vdots \\ \rho \mathcal{D}_N \frac{\partial c_N}{\partial r} \end{bmatrix}, \quad \mathbf{G}_v = \begin{bmatrix} 0 \\ \tau_{rz} \\ \tau_{zz} \\ U_r \tau_{rz} + U_z \tau_{zz} - q_z \\ \rho \mathcal{D}_1 \frac{\partial c_1}{\partial z} \\ \vdots \\ \rho \mathcal{D}_N \frac{\partial c_N}{\partial z} \end{bmatrix}. \quad (12)$$

Here, r , z , and θ are the radial, axial, and azimuthal coordinates of the axisymmetric frame, U_r and U_z are the radial and axial velocity components, g_z is the acceleration due to gravity (assumed to have only an axial component here), q_r and q_z the radial and axial components of the heat flux, and τ_{rr} , τ_{rz} , τ_{zz} , and $\tau_{\theta\theta}$ are the components of the viscous fluid stresses.

B. Thermodynamic and Transport Properties

Expressions for individual species and mixture thermodynamic and transport properties are required to complete the system of partial differential equations for the reactive mixture given above. The empirical expressions compiled by Gordon and McBride^{14,15} are used to specify the h_s and the species specific heat, $c_{p,s}$, entropy, Δs_s , viscosity, μ_s , and thermal conductivity, κ_s , as functions of temperature. The Gordon-McBride dataset contains curve fits for over 2000 substances, including 50 reference elements. For example, the enthalpy for a particular species, h_s , is given by

$$h_s = R_s T \left[-a_{1,s} T^{-2} + a_{2,s} T^{-1} \ln T + a_{3,s} + \frac{a_{4,s} T}{2} + \frac{a_{5,s} T^2}{3} + \frac{a_{6,s} T^3}{4} + \frac{a_{7,s} T^4}{5} + b_1 T^{-1} \right] + \Delta h_{f_s}^o, \quad (13)$$

where $a_{i,s}$ and b_1 are the coefficients for the fit and $\Delta h_{f_s}^o$ is the heat of formation for species s . Note that the enthalpy, h_s , defined here is the absolute enthalpy (as opposed to the sensible enthalpy) and includes the heat of formation, $\Delta h_{f_s}^o$, for the species. Perfect mixture rules are then used to determine the thermodynamic properties of the reactive mixture and Wilke's¹⁷ and Mason and Saxena's¹⁸ mixture rules are used to evaluate the mixture viscosity and thermal conductivity, respectively. The species diffusion coefficients, \mathcal{D}_s are calculated by additionally specifying a Schmidt number, $Sc_s = \mu/\rho \mathcal{D}_s$ for each species.

C. Reduced Chemical Kinetic Scheme

In order to demonstrate the validity of the proposed parallel AMR algorithm, numerical results are described herein for the prediction of methane-air laminar flames. Although several detailed chemical reaction

mechanisms are available for describing methane-air combustion processes (e.g., refer to the GRI-Mech 3.0 chemical kinetic model¹⁹), for the algorithm validation, a simplified six-species two-step reduced chemical reaction mechanisms is used as described by Westbrook and Dryer.¹⁶ In this two-step mechanism, methane oxidation is represented as follows:



with empirically derived reaction rates for both reactions. The six species considered are methane (CH_4), oxygen (O_2), carbon dioxide (CO_2), carbon monoxide (CO), water (H_2O), and nitrogen (N_2). The nitrogen is assumed to be inert. Further details and reaction rates for this reduced mechanism are given by Westbrook and Dryer.¹⁶

III. Parallel AMR Algorithm

A. Finite-Volume Scheme

The flow equations governing a reactive mixture given by Eq. (8) are solved by applying a finite-volume technique in which the mixture conservation equations are integrated over quadrilateral cells of a body-fitted multi-block quadrilateral mesh. The finite-volume formulation applied to cell (i, j) is given by

$$\frac{d\mathbf{U}_{i,j}}{dt} = -\frac{1}{A_{i,j}} \sum_{\text{faces},k} \vec{\mathbf{F}}_{i,j,k} \cdot \vec{\mathbf{n}}_{i,j,k} \Delta\ell_{i,j,k} + \frac{1}{r_{i,j}} \mathbf{S}_{a_{i,j}} + \mathbf{S}_{i,j}, \quad (16)$$

here $\vec{\mathbf{F}} = (\mathbf{F} - \mathbf{F}_v, \mathbf{G} - \mathbf{G}_v)$, $r_{i,j}$ and $A_{i,j}$ are the radius and area of cell (i, j) , and $\Delta\ell$ and $\vec{\mathbf{n}}$ are the length of the cell face and unit vector normal to the cell face or edge, respectively. For the time-invariant calculations performed as part of this study, the optimally-smoothing multi-stage schemes developed by van Leer *et al.*²⁰ are used to integrate the set of ordinary differential equations that arises from this finite-volume discretization procedure. To cope with numerical stiffness, a semi-implicit treatment is used in the temporal discretization of the source terms associated with axisymmetric geometry, finite-rate chemistry, and gravitational acceleration.

The inviscid component of the numerical fluxes at the faces of each cell, $(\mathbf{F}, \mathbf{G}) \cdot \vec{\mathbf{n}}$, are determined from the solution of a Riemann problem. Given the left and right solution states, \mathbf{U}_l and \mathbf{U}_r , at the cell interfaces, the numerical flux is given by

$$(\mathbf{F}, \mathbf{G}) \cdot \vec{\mathbf{n}} = \mathcal{F}(\mathbf{U}_l, \mathbf{U}_r, \mathbf{n}), \quad (17)$$

where the numerical flux \mathcal{F} is evaluated by solving a Riemann problem in a direction defined by the normal to the face with initial data \mathbf{U}_l and \mathbf{U}_r . The left and right solution states are determined using the least-squares piece-wise limited linear solution reconstruction procedure of Barth.²¹ The modified limiter of Venkatakrishnan²² has also been implemented. An extension of the approximate linearized Riemann solver of Roe²³ that accounts for variations in the mixture composition is used to solve the Riemann problem at each cell face and determine the upwind-biased value for \mathcal{F} . An approximation for the Roe-averaged solution state is used that involves the mass weighting of the species mass fractions. The viscous component of the cell face fluxes, $(\mathbf{F}_v, \mathbf{G}_v) \cdot \vec{\mathbf{n}}$, are evaluated by employing a centrally-weighted diamond-path reconstruction procedure as described by Coirier and Powell.²⁴

B. Local Preconditioning

The finite-volume scheme described above is a fully compressible formulation that can readily accommodate large density variations and thermoacoustic phenomena (the latter will be the focus of future studies by the

authors). Nevertheless, laminar combusting flows are in general characterized by very low Mach numbers ($M < 0.2$) and nearly incompressible behaviour. The direct application of unmodified compressible flow solvers to nearly incompressible flows can lead to several numerical difficulties related to disparities between the convective and acoustic propagation speeds (i.e., $|\mathbf{u}| + a \gg |\mathbf{u}|$, where a is the sound speed). The numerical difficulties include slow convergence rates and excessive numerical dissipation. To circumvent these difficulties, a local preconditioning technique proposed by Weiss and Smith^{25,26} is used here to remove numerical stiffness and maintain solution accuracy for low-Mach-number flows.

The preconditioned form of the Navier-Stokes equations for the reactive mixture can be written as

$$\mathbf{\Gamma} \frac{\partial \mathbf{U}}{\partial t} + \frac{\partial \mathbf{F}}{\partial r} + \frac{\partial \mathbf{G}}{\partial z} = \frac{\partial \mathbf{F}_v}{\partial r} + \frac{\partial \mathbf{G}_v}{\partial z} + \frac{\mathbf{S}_a}{r} + \mathbf{S} \quad (18)$$

where $\mathbf{\Gamma}$ is the Weiss-Smith preconditioning matrix for the conserved variable system. The preconditioning matrix reduces the spread of the eigenvalues and improves the numerical solution in the low-Mach number limit. Note that the steady state solution is unaffected by the preconditioning procedure. Details of the preconditioner and eigenstructure of the preconditioned equations are given in the papers by Weiss and Smith²⁵ and Turkel.²⁶

C. Block-Based Adaptive Mesh Refinement (AMR)

Following the approach developed by Groth *et al.* for computational magnetohydrodynamics,^{9,10} a flexible block-based hierarchical data structure has been developed and is used in conjunction with the finite-volume scheme described above to facilitate automatic solution-directed mesh adaptation on multi-block quadrilateral mesh according to physics-based refinement criteria. The proposed AMR formulation borrows from previous work by Berger and co-workers,^{1,2,7,8} Quirk,^{3,6} and De Zeeuw and Powell⁵ for Cartesian mesh and has similarities with the block-based approaches described by Quirk and Hanebutte⁶ and Berger and Saltzman.⁷ Aspects of the block-based adaptive mesh refinement algorithm and parallel implementation for multi-block quadrilateral mesh are described in the recent work by Sachdev *et al.*¹¹ Note that Other researchers have considered the extension of Cartesian mesh adaptation procedures to more arbitrary quadrilateral and hexagonal mesh. See for example the work by Davis and Dannenhoffer²⁷ and Sun and Takayama.²⁸

In this work, the governing equations are integrated to obtain area-averaged solution quantities within quadrilateral computational cells and these cells are embedded in structured blocks consisting of $N_x \times N_y$ cells, where N_x and N_y are even, but not necessarily equal integers. Mesh adaptation is accomplished by the dividing and coarsening of appropriate solution blocks. A hierarchical tree-like data structure is used to keep track of mesh refinement and the connectivity between solution blocks. In regions requiring increased cell resolution, a “parent” block is refined by dividing itself into four “children” or “offspring”. Each of the four quadrants or sectors of a parent block becomes a new block having the same number of cells as the parent and thereby doubling the cell resolution in the region of interest. This process can be reversed in regions that are deemed over-resolved and four children are coarsened into a single parent block. The mesh refinement is constrained such that the grid resolution changes by only a factor of two between adjacent blocks and the minimum resolution is not less than that of the initial mesh. Standard multigrid-type restriction and prolongation operators are used to evaluate the solution on all blocks created by the coarsening and division processes, respectively. Refinement criteria based on a combination of the gradients of the mixture temperature and species mass fractions provide reliable detection of flame fronts.

Solution information is shared between adjacent blocks having common interfaces by employing an additional two layers of overlapping “ghost” cells on each block, which contain solution information from neighbouring blocks. Additional inter-block communication is also required at interfaces with resolution changes to strictly enforce the flux conservation properties of the finite-volume scheme.^{1,2} In particular, the interface fluxes computed on more refined blocks are used to correct the interface fluxes computed on coarser neighbouring blocks and ensure the solution fluxes are conserved across block interfaces.

D. Parallel Implementation

The multi-block quadrilateral mesh and tree data structure lends itself naturally to domain decomposition and enables efficient and scalable implementations of the solution algorithm for the reactive mixture conservation equations on distributed-memory multi-processor architectures.¹¹ A parallel implementation of the block-based AMR scheme has been developed using the C++ programming language and the MPI (message passing interface) library.²⁹ Domain decomposition is carried out by farming the solution blocks out to the separate processors, with more than one block permitted on each processor. For homogeneous architectures with multiple processors all of equal speed, an effective load balancing is achieved by exploiting the self-similar nature of the solution blocks and simply distributing the blocks equally among the processors. For heterogeneous parallel machines, such as a network of workstations and computational grids, a weighted distribution of the blocks can be adopted to preferentially place more blocks on the faster processors and less blocks on the slower processors. Inter-processor communication is mainly associated with block interfaces and involves the exchange of ghost-cell solution values and conservative flux corrections at every stage of the multi-stage time integration procedure. Message passing of the ghost-cell values and flux corrections is performed in an asynchronous fashion with gathered wait states and message consolidation.

IV. Numerical Validation

Initial validation of the proposed parallel AMR scheme is carried out by considering the numerical predictions for two classical non-reacting flow problems and one reactive flow problem. The solutions for these problems are well established and can be used to assess the validity and accuracy of the scheme.

A. Planar Couette Flow

The computation of laminar flow in a channel with a moving wall is used to demonstrate the accuracy of the viscous spatial discretization scheme. Classical planar Couette flow,³⁰ is considered with an upper wall velocity of 29.4 m/s and a favourable pressure gradient of 635.54 Pa. The predicted x-direction velocity component is plotted and compared to the exact analytic solution for this incompressible isothermal flow in Figure 1(a). The L_1 - and L_2 -norms of the solution error are plotted in Figure 1(b). The slopes of the L_1 - and L_2 -norms are 2.03 and 2.04 respectively, indicating that the scheme is indeed second-order accurate.

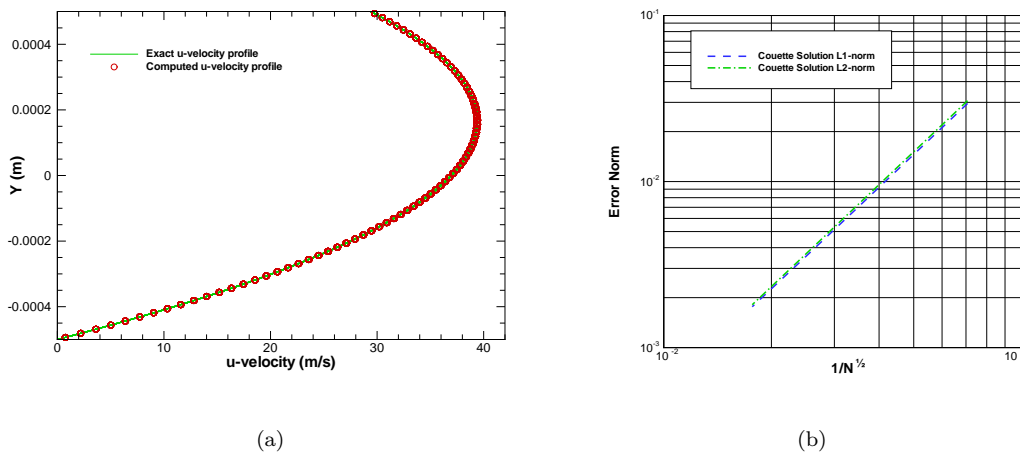
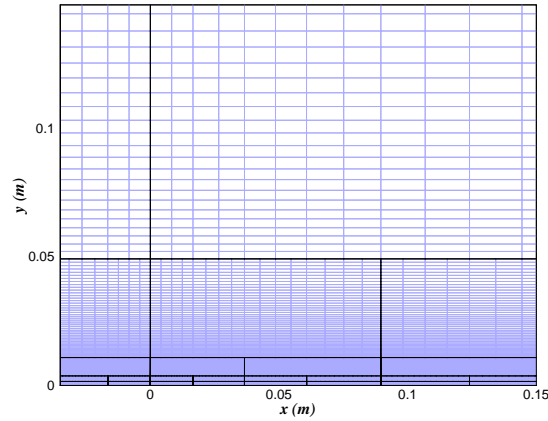


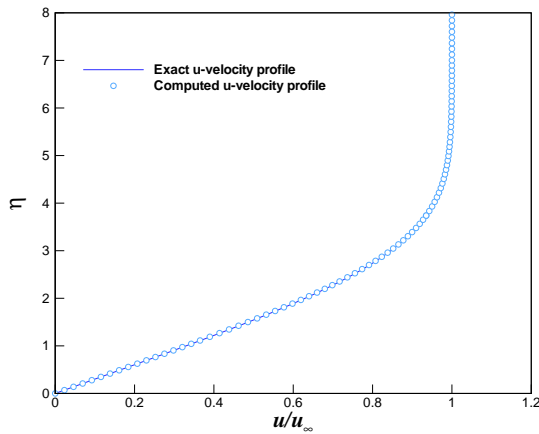
Figure 1. Laminar Couette Flow: (a) u-velocity profile (1 block and 3200 cells), (b) L_1 - and L_2 -norms of the solution error.

B. Laminar Flat Plate Boundary Layer Flow

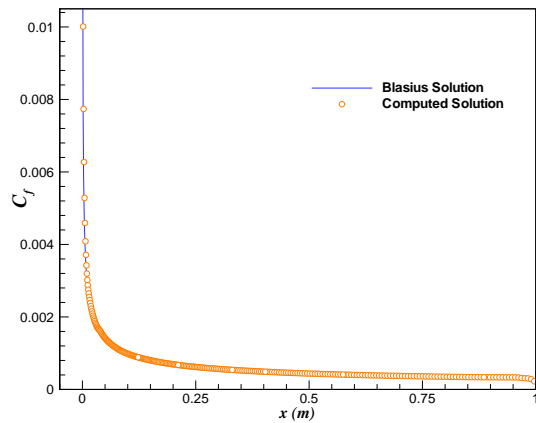
The computation of laminar flow over a flat plate at zero incidence is considered to further demonstrate the accuracy of the viscous spatial discretization procedure. The free-stream Mach number and Reynolds number, based on the length of the plate, for the case considered are $M = 0.2$ and of $Re = 10,000$, respectively. The exact solution of the incompressible boundary layer equations first obtained by Blasius is given by Schlichting.³¹ The calculated boundary layer solution is shown in Figure 2. The mesh consisting of 92 blocks and 70,656 cells is shown in Figure 2(a) for the leading edge region of the plate. Note the anisotropic non-uniform mesh spacing for this case. The first node normal to the plate is located at a distance of approximately $3 \times 10^{-5}m$. The prediction of the non-dimensional x-direction velocity component and the skin friction coefficient are shown in Figures 2(b) and 2(c). The x-direction velocity component is plotted at $Re_x = 8000$. It can be seen that the x-direction velocity component and the skin friction coefficient are in excellent agreement with the Blasius solution, providing further validation of the schemes accuracy.



(a)



(b)



(c)

Figure 2. Laminar flat plate boundary layer: (a) Body-fitted mesh at the leading edge (92 blocks and 70,656 cells), (b) Non-dimensional velocity components at $Re_x = 8000$, and (c) Estimation of the skin friction coefficient.

C. Premixed Laminar Flame

Validation of the proposed parallel AMR scheme for laminar reacting flows is carried out by considering the numerical predictions of planar one-dimensional premixed methane-air flames for a range of equivalence ratios and comparing the predictions to those obtained using the CHEMKIN program PREMIX. The six-species, two-step, reduced kinetic scheme for the oxidation of methane described above is used in all cases. CHEMKIN is a commercial software tool available from Reaction Design for solving complex chemical kinetics problems and PREMIX is a utility that can be used for predicting one-dimensional premixed flames. A detailed 17-species, 58-reaction kinetic scheme is used in the PREMIX calculations to represent the oxidation of methane. These comparisons provide a check of the algorithms ability to predict two key features of laminar flames: the flame temperature and laminar flame speed.

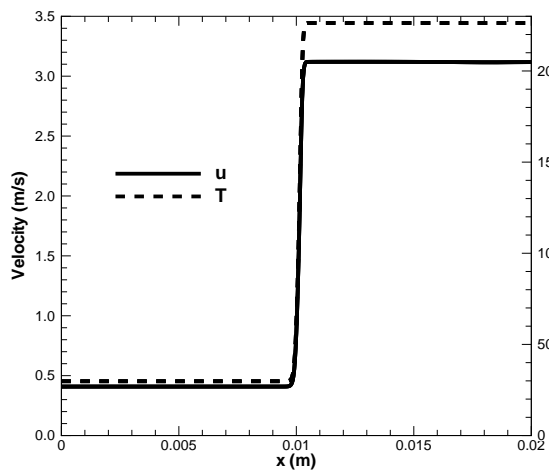
For the premixed flame predictions, a fixed (non-adapted) one-dimensional mesh with 100 non-uniformly space computational cells is used. The steady state or time-invariant structure of the flame is then obtained by starting with uniform fresh and burnt gas solution states at atmospheric and the adiabatic flame temperatures, respectively, and iterating until a steady-state solution is achieved with a stationary flame structure. The upstream and downstream boundary velocity and pressure are adjusted such that the mass flux is constant throughout the domain.

The numerical results for the premixed laminar flame are summarized in Figures 3(a), 3(b), 3(c) and Table 1. The table gives predictions of both the equilibrium temperature of the products, T , and the laminar flame velocity, s_L , as a function of the equivalence ratio ($\phi = 0.6, 0.8, 1.0$, and 1.2 are considered). The overall agreement between the two sets of results is very good, especially considering that the six-species two-step chemical kinetics scheme used by the parallel solver is greatly simplified in comparison to the 17-species, 58-reaction scheme used in the CHEMKIN calculations. This provides strong support for the validity of the proposed reactive flow solver. The two figures provide further evidence. They depict the predicted flame structure for $\phi = 1$ and show variation of the velocity, temperature, and mass fraction through the flame. The predicted laminar flames speed is $s_L = 40.6$ cm/s in this case and the temperature of the products (flame temperature) is $T = 2256$. Both of these values are in good agreement with the predicted values of CHEMKIN. Note that for a stoichiometric mixture with $\phi = 1$, the mass fractions of the fresh gas mixture are: $c_{\text{CH}_4} = 0.0551$, $c_{\text{O}_2} = 0.2202$, $c_{\text{N}_2} = 0.7247$, $c_{\text{CO}_2} = 0$, $c_{\text{CO}} = 0$, and $c_{\text{H}_2\text{O}} = 0$.

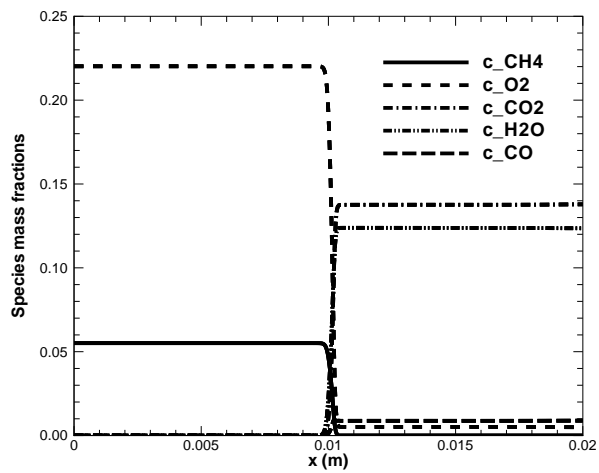
It should be noted that the flow Mach numbers for the premixed laminar flames are very small ($M \approx 0.001 - 0.003$) and the low-Mach-number preconditioning is absolutely necessary for these cases in order to get accurate predictions of the flame structure with the proposed compressible finite-volume formulation. Moreover, the preconditioning compressible equations permit an accurate calculation of the pressure jump across the flame, which was found to be about 1.24 Pa, as shown in Figure 3(c), for the $\phi = 1$ case.

	Solution Method	Equivalence Ratio, ϕ			
		0.6	0.8	1.0	1.2
T (K)	PREMIX	1656	1993	2234	2143
	Current	1650	1995	2256	2221
s_L (cm/s)	PREMIX	12.15	29.1	41.0	38.6
	Current	13.3	29.4	40.6	38.5

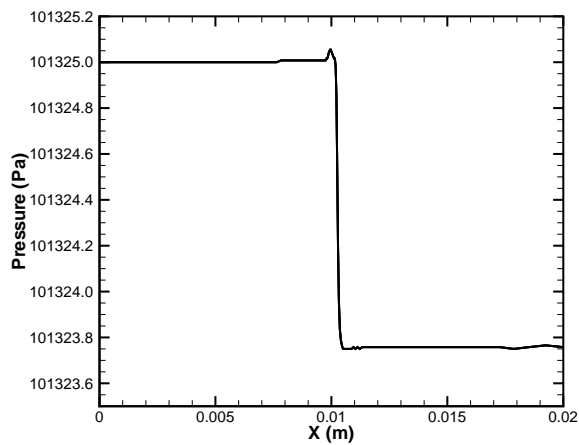
Table 1. Comparison of the predictions of the parallel AMR algorithm using the two-step methane reduced mechanism to those of the CHEMKIN PREMIX program with detailed chemistry for various equivalence ratios. Predictions of both the equilibrium temperature of the products, T , and the laminar flame velocity, s_L , are shown for $\phi = 0.6, 0.8, 1.0$, and 1.2 .



(a) Velocity and Temperature distributions



(b) Species mass fraction distributions



(c) Pressure drop across flame front

Figure 3. Solution of steady one-dimensional premixed methane-air flame structure for $\phi = 1$.

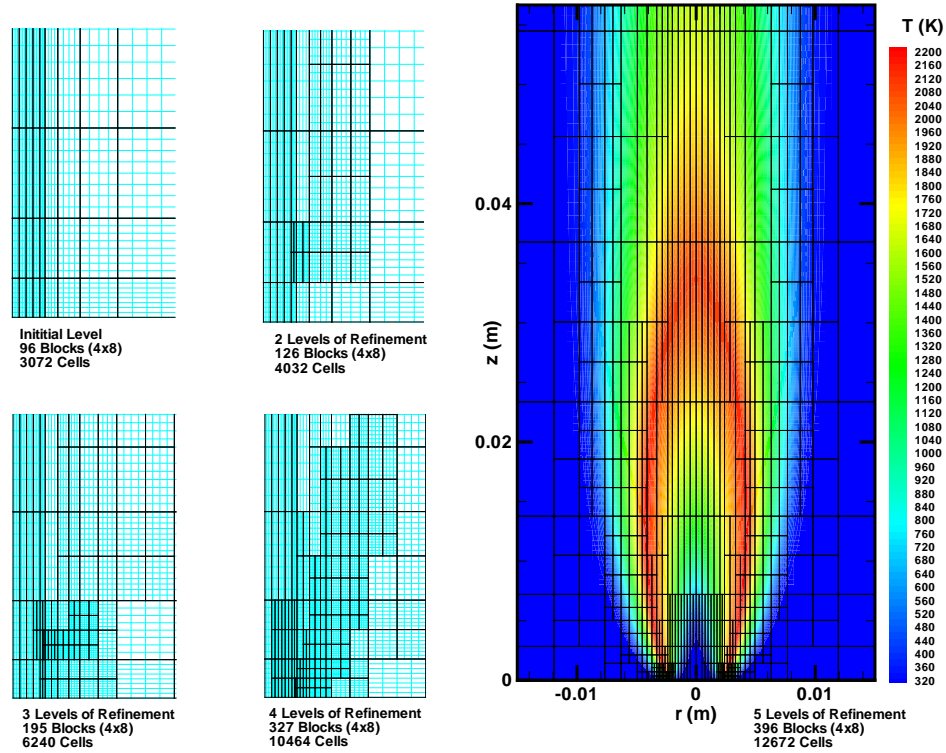


Figure 4. Solution of methane-air axisymmetric laminar diffusion flame showing the computed isotherms and flame structure obtained for a 396 block mesh with 12,672 cells and five levels of refinement. The sequence of adaptively refined grids, showing both the solution blocks and computational cells, is also shown in the figure.

V. Numerical Results

Numerical results are now described for a non-premixed methane-air laminar co-flow axisymmetric diffusion flame. The diffusion flame calculations were carried out on a Beowulf-class parallel computing cluster consisting of 26 4-way Hewlett-Packard Alpha ES40 and ES45 SMP servers with 104 processors and 126 Gbytes of distributed memory. A low-latency Myrinet network and switch is used to interconnect the cluster servers. The six-species, two-step, reduced kinetic scheme for the oxidation of methane is again used for the diffusion flame calculations.

A. Non-Premixed Laminar Diffusion Flame

The parallel AMR method is applied to the solution of an axisymmetric co-flow methane-air diffusion flame. In particular, a solution of the steady laminar flame studied by Mohammed *et al.*³² and Day and Bell¹² is considered. The flame boundary and initial conditions are the same as those used in the previous studies. The computational domain is rectangular in shape with dimensions of 10 cm by 5 cm. The axis of symmetry is aligned with the left boundary of the domain and the right far-field boundary is taken to be a free-slip boundary along which inviscid reflection boundary data is specified. The top or outlet of the flow domain is open to a stagnant reservoir at atmospheric pressure and temperature and Neumann-type boundary conditions are applied to all properties except pressure which is held constant. The bottom or inlet is

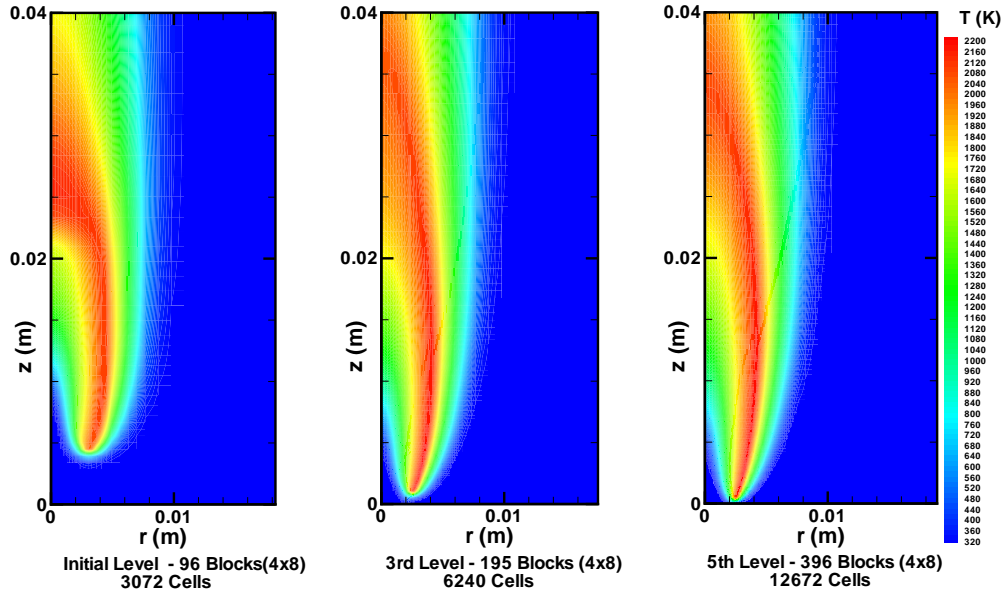


Figure 5. Predicted laminar diffusion flame temperature (K) comparison for 3 different levels of mesh refinement.

subdivided into four regions. The innermost region ($r \leq 2$ mm) is the fuel inlet, which injects a nitrogen diluted methane fuel mixture ($c_{\text{CH}_4} = 0.5149$, $c_{\text{N}_2} = 0.4851$, $c_{\text{O}_2} = 0$, $c_{\text{CO}_2} = 0$, $c_{\text{CO}} = 0$, and $c_{\text{H}_2\text{O}} = 0$) at 298 K with a parabolic velocity profile having a maximum velocity of 0.7 m/s. The next region ($2 \text{ mm} < r \leq 2.38$ mm) is a small gap associated with the annular wall separating the fuel and oxidizer. The third region ($2.38 \text{ mm} < r \leq 2.50$ cm) is the co-flowing oxidizer, in this case air at 298K ($c_{\text{O}_2} = 0.232$, $c_{\text{N}_2} = 0.768$, $c_{\text{CH}_4} = 0$, $c_{\text{CO}_2} = 0$, $c_{\text{CO}} = 0$, and $c_{\text{H}_2\text{O}} = 0$), with a uniform velocity profile of 0.35 m/s. The final outer region of the lower boundary ($2.5 \text{ cm} < r \leq 5$ cm) is again a far-field boundary along which free-slip boundary conditions are applied. The solution domain is initialized with a uniform solution state corresponding to quiescent air at 298K, except for a thin region across the fuel and oxidizer inlets, which is taken to be air at 1500 K so as to ignite the flame. Note that the Mach and Reynolds number based on the fixed diluted methane flow in the fuel inlet are $M = 0.0016$ and $Re = 169$. Additional details concerning the setup for this diffusion flame can be found in the papers by Mohammed *et al.*³² and Day and Bell.¹²

The predicted solution for the laminar diffusion flame obtained using the parallel AMR method is shown in Figure 4. The figure shows the computed isotherms and flame structure obtained using a 396 block mesh with 12,672 cells and five levels of refinement. The sequence of adaptively refined grids, showing both the solution blocks and computational cells, is also shown in Figure 5. The effect of the finer resolution can be clearly seen, as the flame structure becomes much sharpened and more resolved. Finally, Figure 6 shows the mass fractions of the combustion products.

A comparison of the results of Figures 4–6 with those given in the previous studies^{12, 32} reveals, that in spite of the inherent simplifications used in the two-step reaction mechanism, the predicted flame structure agrees very well with the previous work. The “wishbone” structure of the high-temperature region is present and the computed lift-off and flame heights are 0.05 cm and 3.3 cm, respectively, with a maximum centre-line temperature of 2080 K. All of these values agree reasonably well with the previously published results. The predicted value of the carbon monoxide, CO, mass fraction concentration at $z = 3$ cm along the centerline is $c_{\text{CO}} = 0.026$ and, considering the limitations of the reduced chemistry mechanism being used, is in reasonable

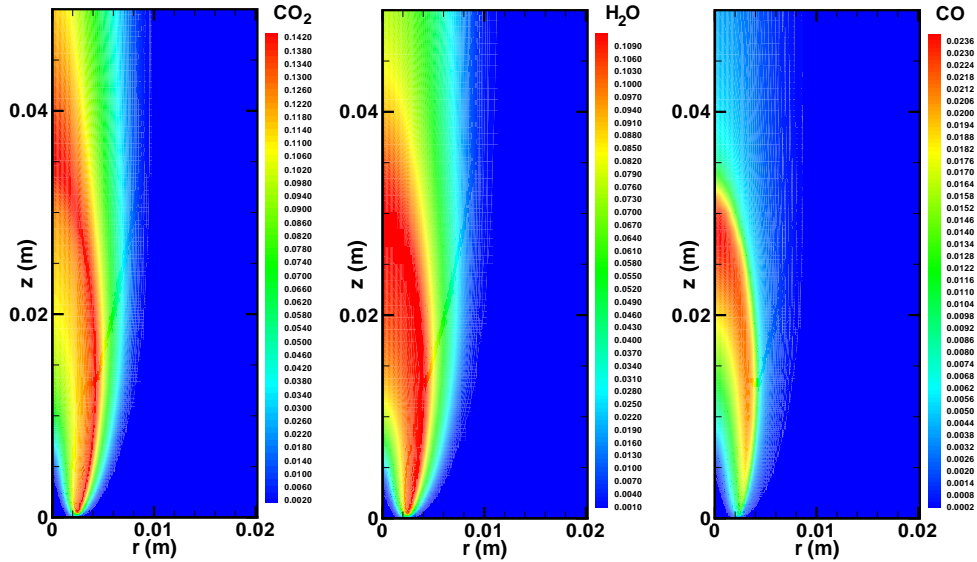


Figure 6. Predicted mass fractions of products CO_2 , H_2O , and CO for laminar diffusion flames.

agreement with those of Mohammed *et al.*,³² who report a mass fraction of $c_{\text{CO}} = 0.03$ at the same location.

B. Parallel Performance

Estimates of the parallel performance and scalability of the proposed solution-adaptive method on the Alpha Beowulf cluster are shown in Figure 7 for a fixed size diffusion flame problem involving 3,200 computational cells (10×10 blocks) and 2,048 cells (8×8 blocks) with 32 solution blocks using up to 32 processors. The figure illustrates both the scaled parallel speed-up, $S_p = (t_1/t_p)p$, and the scaled parallel efficiency, $E_p = (S_p/p)$, for the problem as a function of the number of processors, p , where t_p is the total processor time required to solve the problem using p processors and t_1 is the processor time required to solve the problem using a single processor. It can be seen that the parallel speed-up of the block-based AMR scheme is linear and is 90% efficient for up to 32 processors using the larger (10×10) solution blocks. For the smaller (8×8) blocks, the efficiency drops slightly down to 80% efficient.

VI. Concluding Remarks

A parallel AMR scheme has been described for solving laminar combusting flows. The combination of finite-volume discretization procedure parallel block-based AMR strategy, and low-Mach-number preconditioning has resulted in a powerful computational tool for predicting a wide range of laminar reactive flows, from compressible to nearly incompressible low-Mach-number regimes. The validity and performance of the method has been demonstrated for both premixed and non-premixed flames. Future work will include the investigation of Newton-Krylov-Schwarz strategies in an effort to improve the efficiency of the time integration procedure while maintaining high parallel efficiency.

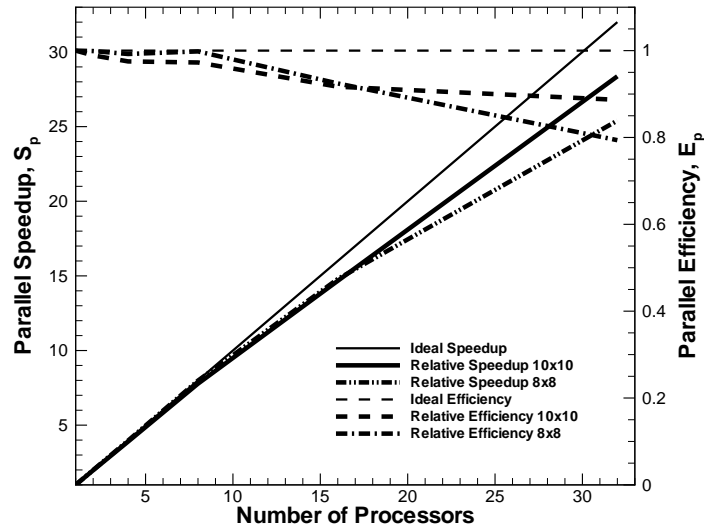


Figure 7. Scaled parallel speed-up, $S_p = (t_1/t_p)p$, and parallel efficiency, E_p , for a fixed-size laminar diffusion flame problem using up to 32 processors.

Acknowledgments

This research was supported by a Premier’s Research Excellence Award from the Ontario Ministry of Energy, Science, and Technology and by the Natural Sciences and Engineering Research Council of Canada (NSERC CRD Grant 254794-01). Funding for the parallel computing facility was obtained from the Canadian Foundation for Innovation and Ontario Innovation Trust (CFI Project No. 2169). The authors are very grateful to these funding agencies for this support. The first author was also supported by a NSERC Postgraduate Scholarship award and wishes to thank the Natural Sciences and Engineering Research Council of Canada for this support.

References

- ¹Berger, M. J., “Adaptive Mesh Refinement for Hyperbolic Partial Differential Equations,” *J. Comput. Phys.*, Vol. 53, 1984, pp. 484–512.
- ²Berger, M. J. and Colella, P., “Local Adaptive Mesh Refinement for Shock Hydrodynamics,” *J. Comput. Phys.*, Vol. 82, 1989, pp. 67–84.
- ³Quirk, J. J., *An Adaptive Grid Algorithm for Computational Shock Hydrodynamics*, Ph.D. thesis, Cranfield Institute of Technology, January 1991.
- ⁴Powell, K. G., Roe, P. L., and Quirk, J., “Adaptive-Mesh Algorithms for Computational Fluid Dynamics,” *Algorithmic Trends in Computational Fluid Dynamics*, edited by M. Y. Hussaini, A. Kumar, and M. D. Salas, Springer-Verlag, New York, 1993, pp. 303–337.
- ⁵De Zeeuw, D. and Powell, K. G., “An Adaptively Refined Cartesian Mesh Solver for the Euler Equations,” *J. Comput. Phys.*, Vol. 104, 1993, pp. 56–68.
- ⁶Quirk, J. J. and Hanebutte, U. R., “A Parallel Adaptive Mesh Refinement Algorithm,” Report 93-63, ICASE, August 1993.
- ⁷Berger, M. J. and Saltzman, J. S., “AMR on the CM-2,” *Appl. Numer. Math.*, Vol. 14, 1994, pp. 239–253.
- ⁸Aftomis, M. J., Berger, M. J., and Melton, J. E., “Robust and Efficient Cartesian Mesh Generation for Component-Based Geometry,” *AIAA J.*, Vol. 36, No. 6, 1998, pp. 952–960.
- ⁹Groth, C. P. T., Zeeuw, D. L. D., Powell, K. G., Gombosi, T. I., and Stout, Q. F., “A Parallel Solution-Adaptive Scheme for Ideal Magnetohydrodynamics,” Paper 99-3273, AIAA, June 1999.

- ¹⁰Groth, C. P. T., De Zeeuw, D. L., Gombosi, T. I., and Powell, K. G., "Global Three-Dimensional MHD Simulation of a Space Weather Event: CME Formation, Interplanetary Propagation, and Interaction with the Magnetosphere," *J. Geophys. Res.*, Vol. 105, No. A11, 2000, pp. 25,053–25,078.
- ¹¹Sachdev, J., Groth, C., and Gottlieb, J., "A parallel solution-adaptive scheme for predicting multi-phase core flows in solid propellant rocket motors," submitted to the International Journal of Computational Fluid Dynamics, September 2003.
- ¹²Day, M. S. and Bell, J. B., "Numerical Simulation of Laminar Reacting Flows with Complex Chemistry," *Combust. Theory Modelling*, Vol. 4, No. 4, 2000, pp. 535–556.
- ¹³Douglas, C. C., Ern, A., and Smooke, M. D., "Numerical Simulation of Flames Using Multigrid Methods," *Iterative Methods in Scientific Computation*, edited by J. Wang, M. B. Allen, B. M. Chen, and T. Mathew, Vol. 4 of *IMACS Series in Computational and Applied Mathematics*, New Brunswick, 1998, pp. 149–154.
- ¹⁴Gordon, S. and McBride, B. J., "Computer Program for Calculation of Complex Chemical Equilibrium Compositions and Applications I. Analysis," Reference Publication 1311, NASA, 1994.
- ¹⁵McBride, B. J. and Gordon, S., "Computer Program for Calculation of Complex Chemical Equilibrium Compositions and Applications II. Users Manual and Program Description," Reference Publication 1311, NASA, 1996.
- ¹⁶Westbrook, C. K. and Dryer, F. L., "Simplified Reaction Mechanisms for the Oxidation of Hydrocarbon Fuels in Flames," *Combust. Sci. Tech.*, Vol. 27, 1981, pp. 31–43.
- ¹⁷Wilke, C. R., "A Viscosity Equation for Gas Mixtures," *J. Chem. Phys.*, Vol. 18, 1950, pp. 517–519.
- ¹⁸Dixon-Lewis, G., "Computer Modeling of Combustion Reactions in Flowing Systems with Transport," *Combustion Chemistry*, edited by W. C. Gardiner, Springer-Verlag, New York, 1984, pp. 21–126.
- ¹⁹Smith, G. P., Golden, D. M., Frenklach, M., Moriarty, N. W., Eiteneer, B., Goldenberg, M., Bowman, C. T., Hanson, R. K., Song, S., Gardiner, W. C., Lissianski, V. V., and Qin, Z., "GRI-Mech 3.0," http://www.me.berkeley.edu/gri_mech/, 2000.
- ²⁰van Leer, B., Tai, C. H., and Powell, K. G., "Design of Optimally-Smoothing Multi-Stage Schemes for the Euler Equations," Paper 89-1933-CP, AIAA, June 1989.
- ²¹Barth, T. J., "Recent Developments in High Order K-Exact Reconstruction on Unstructured Meshes," Paper 93-0668, AIAA, January 1993.
- ²²Venkatakrisnan, V., "On the Accuracy of Limiters and Convergence to Steady State Solutions," Paper 93-0880, AIAA, January 1993.
- ²³Roe, P. L., "Approximate Riemann Solvers, Parameter Vectors, and Difference Schemes," *J. Comput. Phys.*, Vol. 43, 1981, pp. 357–372.
- ²⁴Coirier, W. J. and Powell, K. G., "Solution-Adaptive Cartesian Cell Approach for Viscous and Inviscid Flows," *AIAA J.*, Vol. 34, No. 5, May 1996, pp. 938–945.
- ²⁵Weiss, J. M. and Smith, W. A., "Preconditioning Applied to Variable and Constant Density Flows," *AIAA J.*, Vol. 33, No. 11, 1995, pp. 2050–2057.
- ²⁶Turkel, E., "Preconditioning Techniques in Computational Fluid Dynamics," *AnnRevFM*, Vol. 31, 1999, pp. 385–416.
- ²⁷Davis, R. L. and Dannenhoffer, J. F., "Decomposition and Parallelization Strategies for Adaptive Grid-Embedding Techniques," *Int. J. Comput. Fluid Dyn.*, Vol. 1, 1993, pp. 79–93.
- ²⁸Sun, M. and Takayama, K., "Conservative Smoothing on an Adaptive Quadrilateral Grid," *J. Comput. Phys.*, Vol. 150, 1999, pp. 143–180.
- ²⁹Gropp, W., Lusk, E., and Skjellum, A., *Using MPI*, MIT Press, Cambridge, Massachusetts, 1999.
- ³⁰Muson, B. R., Young, D. F., and Okiishi, T. H., *Fundamentals of Fluid Mechanics*, Wiley, 3rd ed., 1998.
- ³¹Schlichting, H., *Boundary-Layer Theory*, McGraw-Hill, Toronto, 7th ed., 1979.
- ³²Mohammed, R. K., Tanoff, M. A., Smooke, M. D., and Long, A. M. S., "Computational and Experimental Study of a Forced, Time-Varying, Axisymmetric, Laminar Diffusion Flame," *Twenty-Seventh Symposium (International) on Combustion*, The Combustion Institute, Pittsburgh, 1998, pp. 693–702.